Reexamining the nuclear structure of ^{154}Gd in the dynamic pairing plus quadrupole model

J. B. Gupta[1,*] and J. H. Hamilton[2]
[1]*Ramjas College, University of Delhi, Delhi-110007, India*
[2]*Physics Department, Vanderbilt University, Nashville, Tennessee 37235, USA*
(Received 15 August 2016; revised manuscript received 19 February 2017; published 5 May 2017)

In a previous study of the collective multiphonon bands in ^{154}Gd, using the microscopic dynamic pairing plus quadrupole model, data for eight K bands were analyzed. In the last four decades, its decay scheme is significantly revised and the nuclear theory has undergone a significant change. Special focus is on new weak intensity transitions in several bands and on the reassigned levels in its decay scheme. The present study represents a detailed revised analysis of the collective even parity bands below 2.1 MeV. Also, a discussion is given on the nature of the $K^\pi = 0^+$ excited bands, validity of band mixing approach, and of the assumption of shape coexistence of β band with ground band. Comparison is made with the $X(5)$ analytical symmetry and the algebraic interacting boson model predictions. Discussion of the $2n$ transfer reactions is given. The validity of the multiphonon view of the $K^\pi = 4^+$ and 2_2^+ bands is also studied.

DOI: 10.1103/PhysRevC.95.054303

I. INTRODUCTION

The nucleus ^{154}Gd is softly deformed, and is one of the four $N = 90$ isotones ($Z = 60-66$), which are considered to be good candidates for the analytically solvable critical point symmetry $X(5)$ [1], lying at the edge of the spherical to deformed or U(5) to SU(3) transition path [2–5]. This nucleus serves as a good laboratory for the study of the multiphonon collective bands in the framework of the unified collective model of Bohr-Mottelson [6], as well as for the algebraic Interacting Boson model (IBM-1 and IBM-2) [7], and microscopic theories. Earlier in (1979), the band structures of ^{154}Gd were studied in the microscopic theory of dynamic pairing plus quadrupole model [8], wherein the decay character of the eight even-parity collective bands of this nucleus were analyzed [9]. Much new data on this nucleus have become available in the last four decades and many new concepts in nuclear theory have evolved meanwhile. Thus a revisit of its structure in the microscopic view, *vis-á-vis* the new data and the current concepts, is warranted.

In the early 1970s, there was much interest in the β-g, γ-g, and γ-β band mixing anomalies (to get consistent band mixing parameter Z_γ and Z_β for a band) in Sm and Gd isotopic chains and other deformed rare earths. The possibly larger $M1$ admixtures in β-g transitions, which could partially resolve these anomalies for β bands, were not found. A review of these anomalies may be seen in Ref. [10]. Sousa *et al.* [11] from ^{154}Tb decay, and Gupta *et al.* [12] from ^{154}Eu decay [using large volume Ge(Li) detectors], extended the study of the nucleus ^{154}Gd to 25 even parity levels below 2.1 MeV, up to $I^\pi \leqslant 6^+$, spread over seven vibrational bands. The understanding of the structure of these multiphonon bands presented a challenge for the collective nuclear theories.

As stated above, the dynamic pairing plus quadruple (DPPQ) model was employed to interpret the multiphonon structures in terms of full β-γ vibration mixings [9]. In that work, besides the six bands, viz. $K^\pi = 0_1^+$ ground band, $K^\pi = 0_2^+$ β band, $K^\pi = 2_1^+$ γ band, $K^\pi = 0_3^+$ $\beta\beta$ band, $K^\pi = 2_2^+$ $\beta\gamma$ band, and $K^\pi = 4_1^+$ $\gamma\gamma$ band, predictions for two other higher excited bands ($\gamma\gamma$ $K^\pi = 0_4^+$, $3\beta = 0_5^+$) were made, for which scanty data were available or no confirmed spin parity was assigned. Static character of two other bands ($\gamma + 2\beta$ $K^\pi = 0_6^+$,$2\gamma + \beta$ $K^\pi = 4_2^+$) were also given. Due to lack of data, some predictions were just based on theory. In the present study, we reexamine the DPPQ model predictions with the presently available data [13,14]. In Sec. II, we review the present experimental information on new data and involving two nucleon transfer reactions. In Sec. III, a brief review of the DPPQ model is given to introduce the basic concepts and the terminology. The interacting Boson model (IBM) is also introduced there. The experimental data are compared with predictions from theory in Sec. IV, where the results are analyzed. A summary is given in Sec. V. For convenience, we use the nomenclature of multiphonon β, γ combinations, even if these need to be justified yet.

II. NEW DATA ON THE LEVEL STRUCTURE OF ^{154}Gd

In the last four decades, with the advances in experimental facilities, especially in the detector technology and computerized multichannel analysis and storing of data, much additional information is available. Very low in energy and/or weak in intensity γ rays have been identified and resolved in the decay scheme of ^{154}Gd. The Nuclear Data Sheets (NDS) 110 of 2009 [14] lists several new transitions in the decay scheme of ^{154}Gd. Also several doubtful placements of transitions have been corrected.

Tonev *et al.* [2] determined the lifetimes of some low spin levels in ^{154}Gd and compared their results with the predictions of $X(5)$ symmetry approximation method. Kulp *et al.* [15] used a high efficiency 8π spectrometer to study the spectrum of ^{154}Gd.

A major change concerns the assignment of the $K^\pi = 0_3^+$ bandhead. From the ^{154}Eu decay, Meyer [16] had assigned the

*jbgupta2011@gmail.com

 ©2017 American Physical Society

1292.7-keV level to 0_3^+ by erroneously assuming a 612-keV γ ray ($I_\gamma < 0.016$). The 612-keV γ ray was not found in [12]. In the ^{154}Tb decay, Sousa *et al.* [11] from the conversion electron data corresponding to a 615-keV $E0$ transition to the 680.7-keV 0_β state assigned a 1295.8-keV level and interpreted it as a 2β phonon bandhead [11]. A state at 1292.7 or 1295.8 keV was not observed in the (d, d') work [17] either, as noted earlier [12].

Kulp *et al.* [15] also excluded the 1292.7- and 1295.8-keV level assignments and instead assigned a new 1182-keV level to 0_3^+. This also led them to question the interpretation of the 0_3^+ state as a good example of a 2β phonon state [11,16]. In view of the importance of this issue, it needs further consideration.

The 2^+ level at 1418.2 keV is invariably included in the $K^\pi = 0_3^+$ band. A strong $E2$ transition (602.7 keV) to the 2_β level was confirmed in coincidence [12] and by $E0$ decay to the 815.5-keV 2_β level. In the singles spectrum too, a 1418.2 transition was seen by Gupta *et al.* [12].

The $I^\pi = 4^+$ member of the 0_3^+ band assigned previously to a 1698.3-keV level in (d, d') work [17] is also ambiguous. Gupta *et al.* [12] did not find any of the reported deexciting γ rays [16] in the singles or coincidence work. Instead of the 1698.3-keV 4^+ level, a 1701-keV level was proposed to be the 4^+ member of this band from the study of decay of ^{154}Tb in Ref. [18]. A detailed analysis for this assignment is given in [15,18]. The study of the nature of the 0_3^+ band is of current interest, in the general context of the 2β phonon band.

Also the assignments of the members of the higher lying 0_4^+ band have ambiguities. A 2081-keV level assigned previously to $(2^+,3,4^+)$ in [11] is now replaced by a 2080.2-keV level assigned to 4^+, belonging to a new 0_4^+ band at 1573.9 keV and a 1716.1-keV 2^+ level [15,13,14]. Here we note that the high resolution spectroscopy has enabled one to distinguish the 2080.230-keV level from the 2080.791-keV $I^\pi = 3^-$ level [13].

The 2277.1-keV (2^+ or 3^+) level, taken as the $I^\pi = 2^+$ member of a $K^\pi = 0_5^+$ band in [9], is replaced by 1775.4-keV $I^\pi = 2^+$ one, built on the band head 0_5^+ at 1650.34 keV [13].

The $I = 2$, 3, and 4 members of the band at the 1531-keV level are firmly assigned and the predominant $K = 2$ character is confirmed from the decay characteristics (see [12]). Kulp *et al.* [15] questioned the multiphonon nature of the $K^\pi = 2_2^+$ $\beta\gamma$ band at 1531 keV. They cited the results of our previous calculation [9] in the DPPQ model with inconclusive arguments and emphasized the need of a fresh analysis [15]. Further, Wu *et al.* [19] studied the issue of anharmonicity of the $K^\pi = 4^+$ $\gamma\gamma$ band in ^{154}Gd and other nuclei of this region. The issue of anharmonicity of the multiphonon bands needs further studies to reach a consistent view of the problem.

Thus these revisions of the level structures require a revisit of the predictions in the microscopic DPPQ model. For the sake of a full view of the nuclear structure of ^{154}Gd, and of the ambiguities described above, we need to present the decay structure of all the known even parity bands below 2.1 MeV in ^{154}Gd, along with information on two nucleon transfer reactions. The partial level structure, as adopted here, is illustrated in Fig. 1(a) (data taken from Refs. [13,14]).

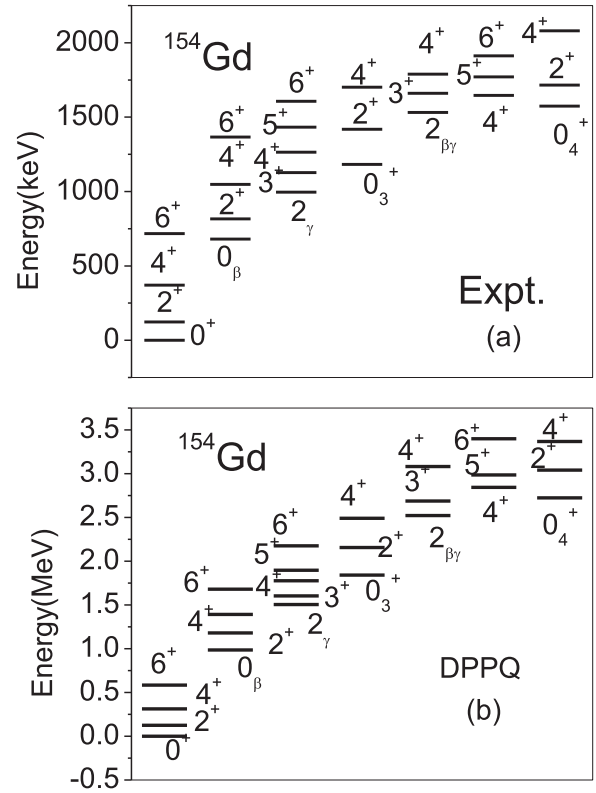

FIG. 1. (a) The partial energy level spectrum in ^{154}Gd [13]. (b) The partial energy level spectrum in ^{154}Gd from DPPQ model.

III. THEORY

A. Microscopic DPPQ model

A detailed description of the Kumar-Baranger method of treating the pairing plus quadrupole model is given in Refs. [20,21], which includes the improvement in the method of solution of the collective Hamiltonian $H_{\rm coll}$, to the original work of Ref. [8] (and the earlier works of Kumar-Baranger). Basically, the DPPQ model is a microscopic theory in the sense that the parameters of the $H_{\rm coll}$ are derived from $H_{\rm PPQ}$, and not obtained *ab initio* by a fit to the experimental data, as done in several other microscopic approaches.

The PPQ Hamiltonian is given by Eq. (1):

$$H_{\rm PPQ} = H_{\rm sph} + H_{\rm Q} + H_{\rm P}. \quad (1)$$

Here $H_{\rm sph} = \Sigma_\alpha\, \varepsilon_\alpha\, c_\alpha^+ c_\alpha$, with ε_α spherical single particle energies of an isotropic harmonic oscillator, and c_α^+, c_α, the spherical harmonic oscillator operators, represent the average spherical field part. The term $H_{\rm Q}$ represents the quadrupole part of the Hamiltonian and $H_{\rm P}$ the monopole pairing part. The quadrupole term includes the quadrupole (particle-hole coupled to $J = 2$, $T = 0$) components of the residual interaction and the pairing term represents the monopole pairing (particle-particle, and hole-hole coupled to $J = 0$ and $T = 1$). Separable Elliot type quadrupole-quadrupole interaction is employed.

A major contribution of Baranger and Kumar to the unification of the spherical vibration and deformed rotation-vibration theory [8] was the adoption of the Hartree-Bogoliubov transformation (HBT) [22] technique in treating the quadrupole

and pairing interaction on equal footing, i.e., the use of the transformation of the spherical single particle operators c_α^+, c_α to deformed quasiparticle operators a_i^+, a_i [Eq. (2)],

$$a_i{}^+ = \sum_\alpha \left(A_\alpha{}^i c_\alpha{}^+ + B_\alpha{}^i c_\alpha\right), \tag{2}$$

where A, B are the wave functions, and for a_i, its complex conjugate (c.c.), a similar expression holds.

The $Z = 40$, $N = 70$ core is treated as an inert core for this region. All the active nucleons over the two major shells of $n = 4$, 5 for protons and $n = 5$, 6 for neutrons are included. The quadrupole strength χ and pairing strengths g_p, g_n are fixed globally for the broad region. Then the deformed quasiparticle energies and wave functions are derived for a mesh of 92 points in the (β,γ) space ($\beta = 0{-}0.5$, and $\gamma = 0^\circ{-}60^\circ$). These are used to derive the seven parameters of the collective Hamiltonian:

$$H_{\rm coll} = V(\beta,\gamma) + T_{\rm vib}(\beta,\gamma) + T_{\rm rot}(\beta,\gamma), \tag{3}$$

where

$$T_{\rm vib}(\beta,\gamma) = \tfrac{1}{2}B_{\beta\beta}(\partial\beta/\partial t)^2 + B_{\beta\gamma}\beta(\partial\beta/\partial t)(\partial\gamma/\partial t) + \tfrac{1}{2}B_{\gamma\gamma}(\beta\partial\gamma/\partial t)^2 \tag{4}$$

and

$$T_{\rm rot}(\beta,\gamma) = \frac{1}{2}\sum_k \theta_k(\beta,\gamma)(\hbar\omega_k)^2, \quad k = 1,2,3. \tag{5}$$

The scalar potential V(β, γ) of Eq. (3), and the other six kinetic terms (three mass parameters $B_{\mu\nu}$ and three moments of inertia θ_k) are derived via the time dependent Hartree-Bogoliubov (TDHB) treatment of the pairing plus quadrupole (PPQ) Hamiltonian [Eq. (1)], as functions of (β,γ). The three moments of inertia $\theta_k(\beta,\gamma)$ are given by

$$\theta_k(\beta,\gamma) = F_B\sum_{ij\tau}(u_i v_j - v_i u_j)^2\langle i|J_k|j\rangle(E_i - E_j)^{-1}. \tag{6}$$

where F_B is the inert core renormalization factor and J_k are the single particle angular momentum operators. The three mass coefficients $B_{\mu\nu}(\beta,\gamma)$ depend on the dynamic treatment of the quasiparticle amplitudes u_i, v_i, quasiparticle energies E_i, and Fermi level λ_τ (see Ref. [20] for the detailed expressions). It employs the cranking formulas.

Also the $E2$, $M1$, and $E0$ operators are determined microscopically. The $H_{\rm xoll}$ are set up and the collective Hamiltonian is solved for each mesh point. Then a summation over the full (β, γ) space provides the dynamics of the Hamiltonian. The DPPQ model includes the dynamics of the five-dimensional quadrupole motion and of the pair fluctuation.

A second unique feature of the dynamic PPQ method is that no fixed shape of the nucleus is assumed. Instead, the nucleus takes it own shape for each spin state. A third speciality is the full (β, γ) freedom of the mass coefficients $B_{\mu\gamma}$ of the kinetic vibration and rotation terms in Eqs. (4) and (5). However, slight variation in the quadrupole strength $\chi = X \times A^{-1.4}$ of the quadrupole interaction in H_Q of Eq. (1) and the value of mass coefficient of the inert core normalization factor F_B for the kinetic energy terms of Eqs. (4) and (5) may be adjusted by a few percent to approximately obtain the $E(2_1^+)$ energy for the given nucleus.

B. Interacting boson model

The interaction boson model (IBM)-1 treats the correlated valence nucleon pairs as proton bosons and neutron bosons equivalently [7]. In IBM-2, the proton bosons and neutron bosons are treated separately. The three limiting symmetries are labeled as U(5), SU(3), and O(6). In the MULT (multipole) form with four terms, $H_{\rm IBM-1}$ can be written as

$$H_{\rm IBM-1} = \varepsilon n_d + kQ\cdot Q + k'L\cdot L + k''P\cdot P. \tag{7}$$

Here the first term represents the boson energy, the second term represents the quadrupole interaction of the $L = 2$ d bosons. The third term represents the O(3) angular momentum contribution, and the fourth term represents the pairing operator interaction. The quadrupole operator is given by

$$Q = (d^+s + s^+d)^{(2)} + \chi(d^+d)^{(2)}. \tag{8}$$

The boson energy operator $n_d = [d^+d]$, $L = \sqrt{10}[d^+ \times d]^{(1)}$, and $P = (1/2)([\tilde{d}\cdot\tilde{d}]{-}[s\cdot s])$.

The coefficients of the four terms are varied to yield the least RMS deviation for the set of input energies (up to 6^+) in experiment. A computer Program PHINT [23] has been used for setting up and solving the IBM Hamiltonian. For ^{154}Gd we set the parameters in Eq. (7) as $\varepsilon = 350$ keV, $2k = QQ = -26.7$ keV, $2k' = \text{ELL} = 12.7$ keV, $k''/2 = \text{PAIR} = 1.9$ keV. For the transition operator $T(E2) = e_B Q$, $e_B = 0.145\,eb$ and $\chi = -0.20/0.145$ was adopted.

IV. COMAPARISON OF DATA WITH THEORY

A. Level structure of ^{154}Gd

The partial level energy spectra of $N = 90$ isotones, depicting the near constancy of (2_g, 4_g, 0_β, and 2_β) energies with varying Z, especially for (Nd, Sm, Gd, and Dy) are illustrated in Fig. 2. These four isotones are considered to be the good examples of the $X(5)$ analytical symmetry [2–5]. The energy of 2_γ varies slightly with proton number Z. The energy difference $E(2_\beta - 0_\beta)$ is almost constant. Also it is almost equal to $E(2_g)$ as apparent in Fig. 3**,** where the $N = 90$ data lie on the diagonal for Ba-Dy ($N = 88{-}96$). (The difference is

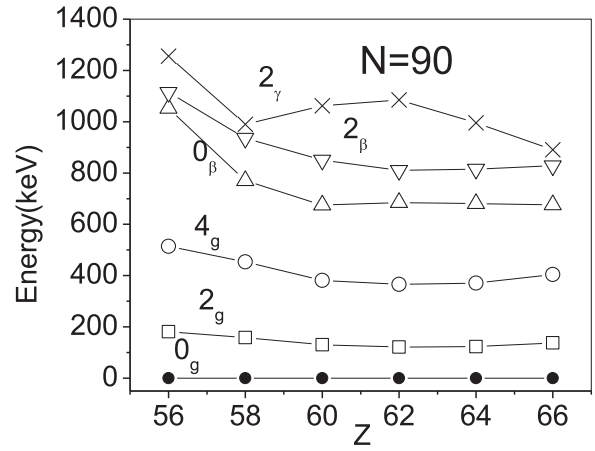

FIG. 2. $N = 90$ energy levels. The $K^\pi = 0_2^+$ bands are well visible. $2_3 = 2_\gamma$ lies above $2_2 = 2_\beta$.

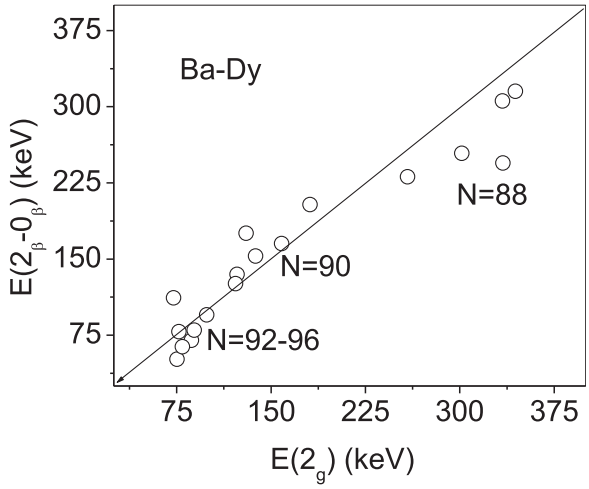

FIG. 3. The energy difference $E(2_\beta\text{-}0_\beta)$ versus $E(2_g)$ for Ba-Dy ($N = 88-96$).The continuous line is the diagonal.

largest for Nd with $E(2_g) = 130$ keV.) The continuous line is the diagonal. Thus the rotational moments of inertia $\theta(=3/E_2)$ of the two bands are almost equal.

The nature of 0_2^+ states in deformed nuclei and of the rotational bands built on them have been the topic of controversy in the last two decades. The proposed shape coexistence of the deformed ground band and vibrational β band in ^{152}Sm led to increased experimental and theoretical activity. Zamfir *et al.* [24] used the IBM prediction of weak $B(E2,2_\gamma \rightarrow 0_\beta)$ as an evidence of the spherical vibrator shape of the β band. The same views are adopted in a review of these issues in Ref. [25]. These views were supported from the large cross section amplitudes obtained in the ^{150}Sm (t, p) reaction, [26], which led to the suggestion that the excited 0^+ states may be spherical vibrational states. Kumar [21] explained the large cross section for $2n$ transfer for the excited state, without assuming a spherical shape in ^{152}Sm. Jolie *et al.* [27] gave a different view on the shape coexistence proposition. Burke [28] analyzed the reasoning cited in [24], based mainly on the weak γ-β $E2$ transition in ^{152}Sm, and pointed out the inconsistency in assuming the shape coexistence. Later, Clark *et al.* [29], using band mixing and the results of the DPPQ model (DPPQM) [21] for ^{152}Sm, obtained results in agreement with experiment and opposed the proposition of shape coexistence in ^{150}Nd and ^{152}Sm. According to recent findings [30], it is explained that a large $2n$ cross section of an excited 0^+ state [26] arises due to the shape difference between the target and the product nucleus. According to DPPQM almost the same deformation is obtained for the three K bands in ^{152}Sm and ^{154}Gd [31,9].

Recently, Gupta and Hamilton [31] reviewed the issue of the nature of $K^\pi = 0_2^+$ bands in deformed nuclei for the $A = 140-180$ region illustrating the universality of β vibration. They illustrated the regularities in the systematics of the level energies and $B(E2)$ values, and explained the experimental fact of $B(E2,0_g \rightarrow 2_\beta)$ being smaller than $B(E2,0_g \rightarrow 2_\gamma)$. A prime cause of this difference is the lesser overlap of the 0_2^+ wave function A_{200} with the ground state wave function A_{100}, leading to smaller intrinsic matrix elements, even if the quadrupole moments are equal. The above cited systematics includes Figs. 2 and 3 here. Further justification based on $B(E2)$ values are given below.

TABLE I. The energy spectrum of ^{154}Gd is compared with the DPPQ model predictions. The level energies are in keV. Only even parity values are calculated.

Band		0^+	2^+	3^+	4^+	5^+	6^+
$K^\pi = 0_1^+$	Expt.	0	123		371		718
	DPPQ	0	126		313		585
$K^\pi = 0_2^+$	Expt.	680	815		1047		1366
	DPPQ	984	1180		1390		1682
$K^\pi = 2_1^+$	Expt.		996	1128	1264	1433	1607
	DPPQ		1505	1602	1776	1895	2178
$K^\pi = 0_3^+$	Expt.	1182	1418		1701		
	DPPQ	1842	2156		2487		
$K^\pi = 2_2^+$	Expt.		1531	1661	1789		
	DPPQ		2520	2688	3084		
$K^\pi = 4_1^+$	Expt.				1646	1770	1912
	DPPQ				2844	2981	3402
$K^\pi = 0_4^+$	Expt.	1574	1716		2080		
	DPPQ	2721	3042		3364		
$K^\pi = 0_5^+$	Expt.	1650	1775				
	DPPQ	2967	3315				

B. K-band structure of the states in ^{154}Gd

The partial energy level spectrum of ^{154}Gd up to $I = 6$ in the lowest seven even parity K bands are illustrated above, in Fig. 1(a). The DPPQ model spectrum is illustrated in Fig. 1(b) and Table I. The spectrum details are given here in reference to their identification in the model calculation. As stated in [9], the energy scale for the calculated vibrational bands is rather expanded [Fig. 1(b)].

The vibrational energy scale may be affected by the pairing strength used here. Also the effect of the spherical single particle energies used is not known. No variation of the inertial factor for the rotation and vibrational terms exclusively is allowed, to maintain the inertia tensor symmetry relations. Recently Li *et al.* [32] studied the effect of the pairing strength in their RMF + BCS treatment of ^{150}Nd using covariant density functional theory. As expected, the increasing pairing strength gave shallower potential energy curve (PEC) minima, and higher $E(0_2^+)$, lower $R_{4/2}$ etc. In DPPQM, on account of the dynamic summation over the whole (β,γ) space, the effects may be more complex. So pairing strength is not varied.

The $K = 0$ and $K = 2$ K-component admixtures predicted in DPPQM for $I = 2$ states of g, β, and γ bands exceed 99%, signifying pure K bands. For $I = 4$ states also, the $K = 0$ components are 99.8%, and 96% in ground and β band respectively. The $K = 2$ component in the 4_3^+ state exceeds 95% with 3.9% $K = 0$ admixture in the γ band. In the following, the numbers in the parentheses for K admixture represent in percent the $K = 0$, $K = 2$ (for $I = 2$) and $K = 4$ (for $I = 4$), and $K = 6$ (for $I = 6$), in that order.

The 2_4^+ state has $(81.4 + 18.6)\%$ $K = 0$ and $K = 2$ admixture associated with the 1418-keV 2^+ level, based on the 1182-keV 0_3^+ 2β band [13–15]. The 4^+ state has $(70 + 22 + 8)\%$ $K = 0, 2$, and 4 admixture which we associate with the newly assigned 1701-keV 4^+ state. The 2_5^+ DPPQM state has $(21 + 79)\%$ $K = 0, 2$ admixture, which we associate with the $K = 2$ $\beta\gamma$ band based on the 1531-keV 2^+ state [13–15]. The sixth 2^+ DPPQM state with $(95.7 + 4.3)\%$ $K = 0, 2$ admixture is associated with the 1716.1-keV state, based on the 1574-keV 0_4^+ state. The seventh 2^+ state in the DPPQM has $(44 + 56)\%$ $K = 0, 2$ admixture.

The fifth 4_5^+ state of the DPPQM (at 2844 keV), with $(22 + 13 + 65)\%$ $K = 0$, 2, and 4 admixture is associated with $K^\pi = 4^+$ $\gamma\gamma$ bandhead at 1645.8 keV. The sixth 4^+ state in DPPQM (at 3084 keV) with $(9 + 63 + 28)\%$ $K = 0$-, 2-, and 4-component admixture corresponds to the 1789.2-keV 4^+ of the $K = 2$ $\beta\gamma$ band. The seventh 4^+ DPPQM state (at 3364 keV) with $(94 + 4 + 2)\%$ $K = 0$, 2, and 4 admixture, is associated with the 2080.2-keV state member of $K^\pi = 0_4^+$ band at 1574 keV. The K components in these states are also useful in determining the degree of band mixing of the collective bands and their identification with respective K bands [Figs. 1(a) and 1(b)].

The second 5^+ of DPPQM (at 2981 keV) has $(57 + 43)\%$ $K = 2$- and 4-component admixture and 5_3^+ (at 3219 keV) has $(40 + 60)\%$ $K = 2, 4$ admixture respectively. The fourth 6^+ in DPPQM (at 2893 keV) has $(64 + 29 + 5 + 2)\%$ $K = 0$-, 2-, 4-, and 6-component admixture. The fifth 6^+ (at 3402 keV) has $(28 + 48 + 21 + 3)\%$ $K = 0, 2, 4$, and 6 admixture, associated with the 1912-keV state. Such large admixtures present the band identity problem.

C. Potential energy surface

In the DPPQ model [20], the potential energy function of the nucleus is given by

$$V(\beta,\gamma) = \sum_{i\tau} v_i^2 \eta_i - \sum_\tau g_\tau^{-1} \Delta_\tau^2 + (1/2)\chi^{-1}\beta^2. \quad (9)$$

Here i represents all the deformed quasiparticle (dqp) states of the two oscillator shells, v_i^2 are the occupation probability of a dqp state, η_i is the dqp energy, g_τ is the pairing strength ($\tau = n, p$), and Δ_τ are the calculated pairing gaps. In the last term, the coefficient $\chi = X \times A^{-1.4}$ (MeV) is the quadrupole force strength. Here we take $X = 70.0$ (a regional value).

The potential energy curve (PEC) $V(\beta,\gamma = 0^\circ)$ in ^{154}Gd from the DPPQ model is depicted in Fig. 4. The $V_{\min}$ lies on the prolate side at $\beta = 0.24$, $\gamma = 0^\circ$, about 3.0 MeV below the spherical barrier at $\beta = 0$. The horizontal line marked as ZPE denotes the zero point energy and lies ~1.8 MeV above the $V_{\min}$. It signifies a spread from $\beta = +0.1$ to $+0.4$, representing softness in the β degree of freedom of the transitional nucleus at $N = 90$. The oblate minimum lies at $\beta = -0.14$ and is only 0.34 MeV deep. The 0.680-MeV 0_2^+, 0.815-MeV 2_β, and 0.996-MeV 2_γ levels lie within the prolate part of the PES. The higher bands are mostly above the spherical barrier and oblate minimum, and hence exhibit considerable mixing of prolate, oblate, and spherical shapes, resulting in large K admixtures.

The PES for ^{154}Gd differs from the infinite square well potential $u(\beta)$ assumed for the $X(5)$ symmetry, with a separation of total $V(\beta,\gamma) = u(\beta) + v(\gamma)$ in [1,2]. In fact the same holds good for the other $N = 90$ isotones as well. The PEC minimum here is not wholly flat and is shifted towards the prolate side significantly. Also there is a contribution of the oblate side, corresponding to $\gamma = 60^\circ$. In view of this, it is rather interesting to predict the properties of the $N = 90$ isotones from the assumptions for $X(5)$ symmetry [2–5]. This difference is not accounted for in the confined βsoft (CBS) model of Pietralla and Gorbachev [33]. First, the CBS model applies to a deformed nucleus lying beyond $X(5)$ towards the rigid deformed limit. Second, it has no $\beta = 0$ part or oblate part, which in fact represent the $\gamma = 60^\circ$ side. The nucleus need not move across the $\beta = 0$ barrier, but can move rather directly along the γ degree of freedom. The β and γ degrees of freedom in a nucleus do not represent independent variables, but are rather coupled. This is apparent on a (β, γ) space diagram for the potential $V(\beta,\gamma)$ as well as for the wave functions of the nuclear collective states. An explicit explanation of this aspect of the PES would be interesting.

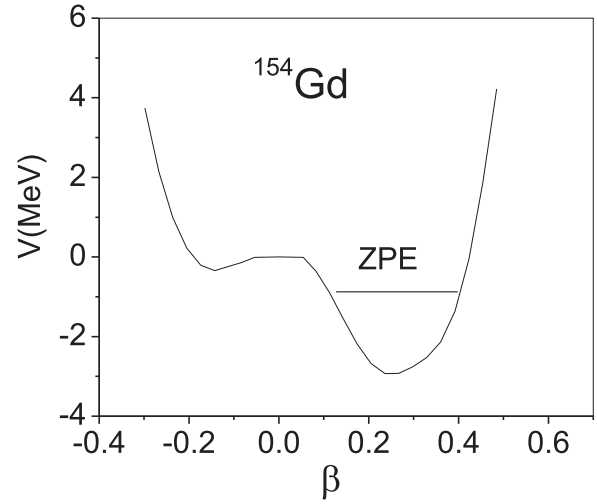

FIG. 4. The potential energy curve $V(\beta,\gamma = 0^\circ)$ in ^{154}Gd from DPPQM. ZPE denotes the zero point energy ~1.8 MeV above the $V_{\min}$.

Using relativistic Hartree-Fock-Bogoliubov (HFB) with nonlinear Lagrangian-3 (NL3) force, Fossion *et al.* [34] illustrated the $V(\beta,\gamma)$ PES for $N = 90$ Nd, Sm, and Gd isotones and noted the difference from the $X(5)$ assumption of a flat square well potential $u(\beta)$. Li *et al.* [35] obtained a similar PES using relativistic energy density functionals (EDFs) for $N = 90$ isotones and noted the difference from $X(5)$ symmetry. Jolie *et al.* [27] using two-parameter $H_{\rm IBM}$ obtained the deformed minimum along with the spherical maximum for ^{152}Sm, as opposed to a double minimum in Ref. [24].

D. $B(E2)$ values and other moments from DPPQM

1. Ground, β, and γ bands

Besides the energy eigenspectrum, the static and dynamic moments and $B(E2)$ values from the model test the validity of the model. Some absolute $B(E2)$ values for the lower

TABLE II. Static moments and absolute $B(E2)$ values (e^2b^2) in ^{154}Gd.

Quantity	Expt. [14,2]	DDM [37]	DPPQ	IBM-1	$X(5)$ [2]
$Q(2_1^+)eb$	−1.82 4	−1.41	−1.79	−1.75	
$Q(2_2^+)eb$			−1.73	−1.24	
$Q(2_3^+)eb$			+1.57	+1.35	
$\mu(2_1^+)\mu n$	+0.91 4	0.93	0.69		
$B(E2,2_1\text{-}0_1)$	0.77 2	0.49[a]	0.772	0.76	0.77[b]
$B(E2,4_1\text{-}2_1)$	1.20 3	0.73[a]	1.163	1.09	1.22
$B(E2,6_1\text{-}4_1)$	1.30 4		1.34	1.17	1.50

[a]If normalized, it yields 0.77 and 1.15.
[b]Normalized value.

three bands are compared with the experimental data in Tables II–V. For the DPPQ model, the quadrupole strength factor X was taken as 70.0 and the inert core renormalization factor $F_B = 2.4$ [9]. The IBM-1 Hamiltonian parameters are given in Sec. III B.

The static quadrupole moment $Q(2_1^+)$ and magnetic moment $\mu(2_1^+)$ (Table II) are in agreement with experiment, providing the first order test of collectivity predicted from theory. Here we note that in the DPPQ model calculation, the electric charge parameter e_n and $e_p = (1 + e_n)$ were kept constant for the whole broad region of rare earths. The same is true for the magnetic moment. The intraband $B(E2)$ values in the ground band also test the validity of the model and indicate the quadrupole collectivity of the nucleus. The normalized value of $X(5)$ symmetry for $I = 4$ also agrees with data. But the $X(5)$ value for $I^\pi = 6^+$ is 15% higher [2] for ^{154}Gd. The same is true for $I = 8$ [2]. Since the $X(5)$ symmetry values do not have a fitting parameter, these deviations indicate its approximations [2] for ^{154}Gd. Also note the almost equal quadrupole moments of the $2_2 = 2_\beta$ and 2_g states in DPPQM. The dynamic deformation model [36] (without any fitting parameters) also yields values [37] in approximate agreement with the data. Our IBM-1 calculation also yields $B(E2)$ values for the ground state band, with deviations increasing with spin. The quadrupole moment of the 2_3^+ state is positive corresponding to the $K = 2$ band.

Absolute $B(E2)$ values for excitation from the ground state (Table III), provide important information regarding the nature of the different excited 2^+ states. The weaker excitation strength of the $K^\pi = 0_2^+$ 2_β state compared to the 2_γ state is a typical feature of their identity. These differences are well given from DPPQM. As cited above, a prime cause of this difference is the lesser overlap of the 0_2^+ wave function A_{200} with the ground state wave function A_{100}, leading to smaller intrinsic matrix elements [31]. In IBM 1 (last column) excitation of 2_β and 2_{03}^+ are weaker (a usual feature of IBM).

From their Coulomb excitation work, Tonev *et al.* [2] quoted $B(E2,0_g \to 2_\beta)$ equal to $0.022(2)\, e^2b^2$. In $X(5)$ symmetry, the normalized value of $0.075\, e^2b^2$ relative to $B(E2,2_g \to 0_g)$ is rather higher by a factor of ∼3. For the fourth 2_4^+ state, a factor of 10^{-3} smaller strength and for the excitation of $2_{\beta\gamma}$ a factor of 10^{-4} weaker strength (Table III) are predicted in the DPPQ model calculation!

Some absolute $B(E2)$ values for transitions from the $K^\pi = 0_2^+$ β band are cited in Table IV. The $B(E2,0_\beta \to 2_g)$ ∼0.26(4) e^2b^2 (average of two values in [9]), or ∼52 W.u. is a good indicator of the collectivity of the β band. This is reproduced in the DPPQ model. The $X(5)$ value (normalized to $B(E2,2_1^+ \to 0_1^+)$ is $0.49\, e^2b^2$ as in Ref. [2]. The values of β-g $B(E2)$ from 2_β, increasing with spins of the ground band,

TABLE III. Absolute $B(E2)$ values (e^2b^2) in ^{154}Gd, for excitation from the ground state.

I_i	I_f	Expt. [2,14]	DPPQ	IBM-1
0_g	2_g	3.85 15	3.86	3.82
	2_β	0.022 2	0.018	0.0025
	2_γ	0.140 8	0.139	0.135
	2_{02}^+		0.0065	0.0035
	$2_{5=\beta\gamma}$		0.0002	

TABLE IV. Absolute $B(E2)$ values (×100) (e^2b^2) from β band in ^{154}Gd.

I_i	I_f	E_γ [13]	Expt. [9][a]	Expt. [2]	DPPQ	$X(5)$ [2]	IBM-1
0_β	2_g	557.6	26 4	22 2	22	49[b]	4[c]
2_β	0_g	815.5	0.48 4	0.45 5	0.37	1.5	0.05[c]
	2_g	692.4	4.0 4	3.3 2	3.3	6.8	1.3
	4_g	444.5	12 1	10 1	8.7	28	2.0
2_β	0_β	134.8	49 16[d]	27.0 18[e]	76	61	51
4_β	2_g	924.5	0.35 8	0.27 2	0.59	0.75	0
	4_g	676.6	3.8 6	2.5 3	3.40	4.4	2.0
	6_g	329.9	11.9 25	7.1 4	8.6	21	1.2
	2_β	232.1	122 35[d]	93 7	120	93	75
6_β	4_g	994.9	0.27 10		0.08		0.02
	6_g	648.3	3.3 10		3.6		2.6
	4_β	318.3			149		85

[a]Values deduced from $B(E2,0_g \to 2_\beta)$ and the $B(E2)$ ratios, in [9].
[b]$X(5)$ values, normalized to $B(E2,2_1^+ \to 0_1^+)$ yield values larger than in experiment. A second alternative is to normalize to $B(E2,0_2^+ \to 2_1^+)$ as done in Ref. [3] for ^{152}Sm.
[c]In IBM-1, β-g transitions are weak.
[d]Reference [38].
[e]Revised value of $B(E2,2_\beta \to 0_\beta)$ from lifetime data [2] seems to lie on the lower side, half of the previous value. It is also far from DPPQM and $X(5)$ values. For ^{152}Sm the value is $> 0.50\, e^2b^2$ [24].

TABLE V. Absolute $B(E2)$ (e^2b^2) × 100 for γ band in ^{154}Gd.

I_i-I_f	E_γ (keV)	Expt. [14]	DPPQ	IBM-1	$X(5)$
2_γ-0_g	996.3	2.86 22	2.78	2.7	2.86[a]
2_γ-2_g	873.2	6.1 5	4.9	4.3	4.3
2_γ-4_g	625.3	0.86 7	0.44	0.65	0.22
2_γ-0_β	315.6	0.08[b]	0.07	0.10	0.25
3_γ-2_g	1004.7		4.5	4.4	5.7
3_γ-4_g	756.8		3.1	3.1	2.4
3_γ-2_γ	131.5		114	99	143
3_γ-2_β	312.3		0.15	0.02	0.33

[a]Normalized to $B(E2,2_\gamma \to 0_g)$ in experiment [39].
[b]Reference [24].

TABLE VI. $B(E2)$ ratios for transitions from $K^\pi = 0_2^+$ β band to ground band in ^{154}Gd. Data taken from National Nuclear Data Center [13,14]. The new transitions, not available previously, are marked by an asterisk.

Transitions		$E_\gamma/E\gamma'$ keV	I_γ/I'_γ	$B(E2)$ ratio	DPPQ	IBM-1	$X(5)$ [2]
2_β	$0_g/2_g$	815.5/692.4	0.2876	0.127 1	0.11	0.04	0.22
815.5	$4_g/2_g$	444.5/692.4	0.3078	2.82 5	2.61	1.60	4.0
	$0_g/4_g$	815.5/444.5	0.934	0.045 2	0.043	0.025	0.056
	$0_\beta/0_g$	134.8*/815.5	0.0156	126 15*	205	1025	40
4_β	$2_g/4_g$	924.6/676.6	0.388	0.081 2	0.18	0	0.16
1047	$6_g/4_g$	329.9/676.6	0.056	2.03 20	2.54	0.62	4.7
	$2_g/6_g$	924.6/329.9	6.93	0.040 5	0.070	0	0.036
	$2_g/2_\beta$	924.6/232.1*	28.5	0.003 1*	0.005	0	0.008
6_β	$4_g/6_g$	994.9/648.3	0.312	0.037 4	0.024	0.008	
1366	$4_g/4_\beta$	994.9/318.3*	0.774	0.0026 3*	0.0005	0.0005	

are also well given in theory [including $X(5)$ and IBM-1]. Also the strong intraband 2_β-0_β transition (old value), only slightly smaller than $B(E2,2_1^+ \to 0_1^+)$ in the ground band, is an indicator of good rotational features of the β band. The same is true for $B(E2,4_\beta \to 2_\beta)$ and $B(E2,6_\beta \to 4_\beta)$. The $B(E2)$ values for transitions from 4_β and 6_β states also are well given in theory.

These results for ^{154}Gd are in agreement with the conclusion by Clark *et al.* [29] for ^{152}Sm in regard to the shape coexistence and also on the nature of the $K^\pi = 0_2^+$ band in $N = 90$ isotones of (Nd-Gd). This also agrees with the observations on the nature of the $K^\pi = 0_2^+$ bands in deformed nuclei reviewed in Ref. [31], but differs from the views based on energy ratio $R_{4/2}$ and (t, p) scattering cross section data and IBM-1 predictions in [24,25]. The energy difference $E(2_\beta\text{-}0_\beta)$ is almost constant for $N = 90$ isotones, Also it is almost equal to $E(2_g)$ as apparent in Fig. 3, where the $N = 90$ data lie on the diagonal for Ba-Dy ($N = 88-96$). The values of $\beta_{\rm rms}$ for the states (up to $I = 6$) of the β band are almost equal to the states in the g band (0.279 versus 0.262 for the 0_2^+ state) (see Table II in [9] for higher states).

The DPPQ model $B(E2)$ values for γ-g $E2$ transitions from 2_γ (Table V) are in good agreement with experimental values. The weak intensity 315.6-keV 2_γ-0_β transition of ~0.17 W.u. [24] (or 0.0008 e^2b^2) is also reproduced in DPPQM and IBM-1. This weak transition led to the anomalous concept of the phase coexistence view in [24], refuted in later works [27–29]. The $B(E2)$ values for transitions from 3_γ are similar in DPPQM, IBM, and $X(5)$, except for $B(E2,3_\gamma\text{-}2_\beta)$.

E. Interband $B(E2)$ ratios

1. $K^\pi = 0_2^+$ β band and $K^\pi = 2^+$ γ band

For proper identification of the energy levels and the deexciting γ rays, the transition energies E_γ and intensities I_γ are also listed in the following tables. In Table VI, we list the revised up-to-date $B(E2)$ ratios for transitions from the $K^\pi = 0_2^+$ β band. The new transitions, not available previously, are marked by an asterisk. The large ratio of intraband to interband transition strengths are well supported by theory. The newly determined $B(E2)$ ratios also agree reasonably well with DPPQ values. For $B(E2,6_\beta \to 4_g/6_g)$, the value is revised from 0.080(30) in [40,9] to 0.037 (4), in better agreement with the DPPQ value. Most of the other DPPQ values are in fair agreement with experiment. Just as for the $N = 90$ isotone ^{152}Sm, the $B(E2)$ ratios for ^{154}Gd from $X(5)$ symmetry also are in fair agreement with data. As stated above, the β-g transitions (especially 2_β-0_g, 4_β-2_g) are weak in IBM-1, which cause larger deviations from data.

Clark *et al.* [29], using the DPPQM results from Kumar's calculation [21] for ^{152}Sm, illustrated the consistent set of β-g $B(E2)$ ratios through band mixing. Similar good agreement with experiment is apparent (Table VI) here for ^{154}Gd, without resorting to the shape coexistence assumption. In fact, in DPPQ model, there is complete freedom of shape dynamically. However, as stated above, no sharp difference in shape between ground and β band is predicted.

The revised values of $B(E2)$ ratios for transitions from the γ band are listed in Table VII along with the old values in [9]. Most values are almost the same, but a few newly measured values, e.g., for 2_γ-$0_\beta/0_g$ and 2_γ-$0_\beta/2_\beta$ differ by almost a factor of 2. For transitions from the 2_γ state, most values are well predicted in DPPQM and IBM-1. The $X(5)$ values for γ-g $B(E2)$ ratios are almost equal to the rotor values. The increased $B(E2,2_\gamma\text{-}0_\beta/0_g)$ [13], nearly double the older value, is not supported in theory. The 3_γ to 4_β transition of 80 keV is weak in DPPQM. Other $B(E2)$ ratios are given reasonably well in theory. For transitions from the higher states of 4_γ, 5_γ, and 6_γ, our theory values are in fair agreement with most data.

2. $K^\pi = 0_3^+$ band

The 0_3^+ at 1182.1-keV and 4^+ at 1701-keV states are the new assignments in this band, and some weak I_γ for the transitions from 1418 keV 2^+ are revised, (see footnote b of Table VIII). Accordingly, several $B(E2)$ ratios in Table VIII are different from the previous values referred to in [9] (columns 4 and 5). For the newly assigned 1182.1-keV 0_3^+ state, the $B(E2,0_3^+\text{-}2_\beta/2_g)$ value of ~40 (in experiment) favors it as collective structure (much larger in theory because of the much weaker $E2$ to 2_g) ($<3 \times 10^{-4}\, e^2b^2$) . The absolute $B(E2,0_3^+ \to 2_\beta) = 0.52\, e^2b^2$ in theory, equivalent to 104 W.u., indicates good collectivity. It is larger than $B(E2,0_\beta \to 2_g) = 0.22(2)\, e^2b^2$. In $N = 90$ isotone ^{152}Sm, $B(E2,0_3^+\text{-}2_\beta/2_g)$ is 43 in experiment and (0.8/0.0064) ~126 in DPPQM, larger by a factor of ~3.

TABLE VII. $B(E2)$ ratios for transitions from $K^\pi = 2_1^+$ γ band in ^{154}Gd.

Transitions I_i I_f/I'_f	$E_\gamma/E\gamma'$ (keV) [13]	I_γ/I'_γ [13]	$B(E2)$ ratios Expt. [9][a]	Expt. [13]	DPPQ	IBM-1	$X(5)$
996.3 keV							
2_γ $4_g/2_g$	625.3/873.2	2.61/100	0.144 5	0.139 2	0.090	0.15	0.052
$0_g/2_g$	996.3/873.2	86.8/100	0.46 1	0.45 1	0.55	0.63	0.66
$0_g/4_g$	996.3/625,3	86.8/2.61	3.3 1	3.3 1	6.1	4.17	1.28
$2_\beta/2_g$	180.7/873.2	0.043/100	1.03 23	1.13 16	1.47	4.1	0.03
$0_\beta/0_g$	315.6/996.3	0.073/86.8	0.14 1	0.26 1	0.03[b]	0.037[b]	0.09
$0_\beta/2_\beta$	315.6/180.7	0.073/0.043	0.063 14	0.104 16	0.010[b]	0.006[b]	1.85
1127.8 keV							
3_γ $2_g/4_g$	1004.7/756.8	100/25.11	1.06 4	0.97 2	1.41	1,42	2.38
$2_\gamma/2_g$	131.5/1004.7	0.073/100	17 1	19 1	26	23	
$4_\beta/2_\beta$	80.4/312.3	0.016/0.101	182 91	140 70	34	694	0.063
$2_\beta/2_g$	312.3/1004.7	0.101/100	0.289 13	0.35 1	0.04[c]	0.01[c]	0.06
$4_\beta/4_g$	80.4/756.8	0.016/25.11	50 25	47 24	1.6[c]	4.2[c]	0.01
1263.8 keV							
4_γ $6_g/4_g$	546.1/892.8	1.68/100	0.27 4	0.20 2	0.37	0.38	0.09
$2_g/4_g$	1140.7/892.8	45.6/100	0.14 1	0.13 1	0.32	0.25	0.31
$2_\beta/2_g$	448.5/1140.7	0.49/45.6	1.15	1.14 17	0.50	0.75	
$2_\gamma/2_g$	267.5/1140.7	1.4/45.6	43.3	43 9	29	33	
1432.6 keV							
5_γ $4_g/6_g$	1061.4/714.9	100/25.5	0.74 15	0.54 2	0.77	0.78	1.67
$4_\gamma/4_g$	168.8/1061.4	5/100	491	<491	19	18	
1606.6keV							
6_γ $4_g/6_g$	1235.1/888.7	43/100	0.08 2	0.08 2	0.14	0.17	0.25

[a]Values adopted in [9] from the weighted average of I_γ in [16] and [41].
[b]Weak $E2$ transition $2_\gamma \rightarrow 0_\beta$ in DPPQM agrees with experiment (Table V), but the $B(E2)$ to 0_g and 2_β are relatively stronger. The same applies to IBM-1.
[c]Again (odd spin) γ-β band mixing is small in DPPQM and much smaller in IBM-1. Also $X(5)$ values [39] differ by large factors.

For the 1418-keV 2^+ state which is well established, preferential decay to β- and γ-band members are also supported in theory, though because of the very weak transition to 2_γ ($4 \times 10^{-5}\, e^2b^2$) in theory, the five $B(E2)$ ratios involving it are larger in theory. The $B(E2, 2^+_{03} \rightarrow 2_\beta) = 0.1\, e^2b^2$ or 20 W.u. in DPPQM indicates a collective $E2$ transition. Most of the other $B(E2)$ ratios are well given in theory. The 1418-keV 2^+_{03} to 0^+_3 125-keV transition, replaced by 236.1-keV intraband transition, yields $B(E2)$ ratio as in theory, indicating a large intraband $E2$ transition. The absolute $B(E2)$ value for this newly assigned intraband transition is predicted to be $0.63\, e^2b^2$, a rotational model value, almost equal to $B(E2, 2_g \rightarrow 0_g) = 0.77\, e^2b^2$ in experiment.

For the 1701-keV 4^+, the weak transition to $4_g (\geqslant 10^{-7}\, e^2b^2)$ and 2_β ($\sim 10^{-5}$) yield large (small) $B(E2)$ ratio in theory. For other transitions, the theory values reproduce the basic pattern of the experimental data. The predicted 80% $K = 0$ admixture and the stronger $E2$ transitions to 4_β, as also given in theory, indicate large band mixing with β band. On account of the 1182-keV 0^+_3 state, yielding energy ratio $E_{03}/E_{0\beta}$ less than 2.0, Kulp *et al.* [15,18] questioned its 2β vibrational character. However, from the general decay pattern of the 0^+_3 and other higher spin members, anharmonic vibration can give a lower energy ratio.

The nature of the second excited 0^+ state of deformed nuclei of this region also has been under discussion for a long time [42,18,30]. Shahabuddin *et al.* (1980) [42] proposed the 1182-keV level of this band in their (t, p) reaction work. On the basis of large $2n$ transfer amplitude, which results from the $\nu[505] \uparrow$ Nilsson intruder orbital, following [42], Kulp *et al.* [18] called this state a "pairing isomer." A pairing isomer implies pairing vibration**,** decoupled from the superfluid ground state. Earlier, Ragnarsson and Broglia [43] noted the larger $\sigma(p,t)$ and small $\sigma(t,p)$ in actinides, and interpreted it as pairing isomer on account of the increased pairing gap Δ, than for the ground state. They explained that the pairing isomers are formed because of the inhomogeneity of oblate and prolate levels in the vicinity of the Fermi surface. However, in ^{154}Gd, the situation is different.

Meyer *et al.* [44] have measured the $2n$ transfer cross section for the (p, t) reaction on ^{152,154}Gd. For ground state (g.s.) to g.s. $2n$ cross section σ, the values are 0.913(4) for ^{152}Gd and 2.37(1) for ^{154}Gd. This supports the interpretation as above [30], in terms of the difference in deformation of the target and the product nucleus. Further, for the 680-keV 0^+_2 in ^{154}Gd, 20% of the ground state σ value is indicated and for the 1182 keV 0^+_3, only a 0.005 fraction is indicated [44].

Using IBM-1 and coherent state formalism, Fossion *et al.* [45], explained the peaks in (t, p) $2n$ transfer cross sections in Gd and other nuclei, and correlated them with the shape phase transition on the U(5) to SU(3) path. They obtained enhanced σ for the excited 0^+_2 state in ^{152}Gd$(t, p)^{154}$Gd reaction using the s^+ operator of IBM. Clark *et al.* [30] reviewed the role of the $2n$ transfer reaction strength for the ground state and excited 0^+

TABLE VIII. $B(E2)$ ratios for transitions from $K^\pi = 0_3^+$ (2β) band at 1182.1 keV 0_3^+ in ^{154}Gd. The DPPQM values for energies are 1842, 2156, and 2487 keV, respectively.

Transitions I_i I_f/I_f'	$E_\gamma/E\gamma'$'(keV) [13]	I_γ/I_γ' [13]	$B(E2)$ ratios Expt. [9,16]	Expt. [13]	DPPQ
1182.1 0_3					
0_3^+ $2_\beta/2_g$	366.6/1059.0	21/100		42 18	1910[a]
1418.1 keV					
2_{03} $2_\beta/2_\gamma$	602.7/421.9	47.7/2.2	>4.8	3.6 28	4.4
$2_\gamma/2_g$	421.9/1295.1	2.2/18.9	>96	32 24	560
$2_\beta/2_g$	602.7/1295.1	47.7/18.9	450	116 11	2470
$4_g/2_g$	1047.2/1295.1	100/18.9	>38	15 1	59
$0_g/2_g$	1417.9/1295.1	13.6/18.9	>1.4	0.5 1	33
$0_\beta/2_\beta$	737.5/602.7	3.7/47.7	0.06 1	0.03 1	0.01
$4_\beta/2_\beta$	370.6/602.7	6.88/47.7	2.0 7	1.6 1	2.7
$0_\beta/0_g$	737.5/1417.9	3.7/13.6	26 5	7.1 14	0.60
$4_\beta/4_g$	370.6./1047.2	6.88/100	20 5	12 1	111
$0_{03}/0_\beta$	236.1/737.5	2.8/3.7	[b]	225 50	810
$0_{03}/2_g$	236.1/1295.1	2.81/8.9	[b]	736 160	1.6×10^4
$2_\gamma/3_\gamma$	421.9/290.4	2.2/2.8	[c]	0.12 10	0.26
1701.4 keV					
4_{03} $4_\beta/4_g$	653.71/330.3[d]	100/75		47[d]	2×10^5
$6_g/4_g$	983.7/1330.3	92/75		5.6	1.0×10^4
$2_\beta/2_\gamma$	885.8/705.1	8.9/2.2		1.3	0.01
$2_\gamma/3_\gamma$	705.1/573.5	2.2/12		0.07	0.26
$2_\gamma/2_g$	705.1/1578.2	2.29/.2		13	5.2
$2_{\beta\beta}/2_\gamma$	283.0/705.1	17/2.2		742	144

[a]The $B(E2,0_3^+ \to 2_g)$ value is of the order of 10^{-4} smaller in theory, unlike the 100 to 21 relative I_γ in experiment [13,14], for the newly assigned 1182-keV 0_3^+ state.
[b]1418-keV 2_{03}^+ to 0_3^+ 125-keV transition is now replaced by 236.1-keV transition.
[c]The 290.4-keV transition to 3_γ is new.
[d]No intensity errors are listed [13] for I_γ from 1701.4-keV state.

states in deformed nuclei, *vis-á-vis* the shape coexistence view and the shape difference of the target and product nucleus. They refuted the assumption of spherical excited state in the product nucleus, based on the earlier interpretations, in [42] and [18]. By comparing with the IBM predictions, they concluded that large σ ($2n$ transfer) for (t, p) and (p, t) reactions arise from the shape difference. This agrees with the results of Ref. [46].

In Ref. [46], the occupation probabilities of protons and neutrons in relevant Nilsson orbits for $N = 88$, 90 isotopes of Gd from DPPQM, were presented (see Tables VII–X and Figs. 5–7 in [46]). A sharp rise of the occupation of $\nu i_{13/2}$ and $\nu h_{9/2}$ down sloping orbitals is indicated, which explains the sharp shape transition at $N = 88-90$, and may give rise to the large $2n$ transfer amplitude, g.s. to g.s., and to the excited states.

Kumar [21] has pointed out for ^{152}Sm that the fluctuations in pairing vibration, giving rise to large $\sigma(t,p)$, should be weak. Also, he noted that there are no two minima in PES corresponding to the excited 0^+ states. However, as illustrated in Fig. 4 for the PES, the multiphonon bands lie above the spherical barrier, hence some reduction in $\beta_{\rm min}$ and $\beta_{\rm rms}$ for these states is possible. Thus, the pairing vibration may contribute simultaneously, to the quadrupole vibration, supported by the $B(E2)$ data (absolute and relative) for the 0_3^+ and higher spin members and the collectivity of the band.

In this context, it is noted that in the present treatment of DPPQM, we have not calculated explicitly the statewise $2n$ transfer cross section for (p, t) and (t, p) stripping and pick up reactions, though we have calculated the occupation probabilities of the individual Nilsson orbits as referred to in the paragraph above. As per Kumar's observation, one needs to estimate the fluctuations in the pairing field and the quadrupole field for individual excited 0^+ states. Kumar [[21], (Table 15)] also estimated the summed up occupation of Nilsson orbits and obtained increased $\sigma(t,p)$ for the excited state in ^{152}Sm. The difference between $\sigma(p,t)$ and $\sigma(t,p)$ can also be on account of the use of v and u probability amplitudes of pairing in the two cases. However, if the change in deformation for excited state is small, this will be difficult to estimate.

3. $K^\pi = 4^+$ band at 1645.8 keV

As stated above, the fifth 4^+ of DPPQM has (22 + 13 + 65)% K = 0-, 2-, and 4-component admixture, which we associate with the 1646-keV state. In the first four rows of Table IX, the $B(E2)$ values for transitions from $I = 4_{\gamma\gamma}$ at 1646 keV to the 996-keV γ band, relative to the 680-keV β band and the g band, are listed, which display the preferential decay to the γ band, rather than to the ($\Delta K = 4$) β band. The ($\Delta K = 4$) transitions to the g band are weaker by two orders

TABLE IX. $B(E2)$ ratios for transitions from $K^\pi = 4_1^+$ $(\gamma\gamma)$ $I = 4$ (1645.8-keV) band in ^{154}Gd.

Transitions I_i I_f/I_f'	$E_\gamma/E\gamma'$ (keV) [13]	I_γ/I_γ' [13]	Expt. [9,11]	Expt. [13]	DPPQ
1646 keV					
$4_{K=4}$ $2_\gamma/2_\beta$	649.6/830.5	100/7.1	57 8	48 5	28
$2_g/2_\gamma$	1522.8/649.6	1.0/100	0.004 1	0.0014 3	0.021
$4_\gamma/4_\beta$	382.0/598.2	10.8/12.0	6.6 10	8.5 16	22
$4_g/4_\gamma$	1275.7/382.0	2/10.8	0.0013	0.0004 4[a]	0.026
$4_{K=4}$-$3_\gamma/2_\gamma$	518.0/649.6	57.0/100	1.72 17	1.77 9	1.29
$4_\gamma/2_\gamma$	382.0/649.6	10.8/100	1.33 22	1.54 6	1.02
$2_\beta/4_\beta$	830.5/598.2	7.1/12.0	0.10 3	0.11 2	0.67
$3_\gamma/4_\gamma$	518.0/382.0	57.0/10.8	1.30 22	1.15 8	1.26
$2_g/4_g$	1522.81/275.7	1.0/2	0.43 15	0.2 2[a]	0.8
$6_g/4_g$	928.2/1275.7	3.4/2	4.9 16	8 8[a]	0.6

[a]For 1275.7 keV, $I_\gamma = 2(2)$ listed in [13,14], indicates 100% error.

of the magnitude (with a large error margin). These features are supported in DPPQM. Also, the other $B(E2)$ ratios involving two levels of the same band in the lower six rows agree with experiment (with one exception).

For the $I = 5$ state at 1770 keV (Table X), the first row displays a factor of 250 stronger decay for the intraband transition [13]. The revised $B(E2)$ ratio for $5_2 \rightarrow 4_\gamma/4_\beta$ of 21(9) again indicates a stronger decay to the γ band. The transition to 4_g is further weakened by a factor of 60 compared to 4_β. In Table X, two sets of values (5_2 and 5_3) of DPPQM are listed. The 5_2^+ state in DPPQM has $(56 + 44)\%$ $K = 2$, 4 components and 5_3^+ has $(40 + 60)\%$ $K = 2$, 4 admixture, indicating good mixing with the $K = 2$ γ-vibration band. The values from 5_2^+ seem to be closer to the data, as in [9], than those from the 5_3^+ state (last column), though its $K = 4$ component admixture is smaller than $K = 2$.

For the 6^+ at 1911.5 keV, strong intraband transition strength and preferential decays to the γ band compared to β band and g band are indicated. The fifth 6^+ DPPQ model values are compared with data. The $B(E2)$ ratios from theory agree with the data in some cases and are far in other cases. The absolute intraband $B(E2)$ value from 6^+ [19] is reproduced approximately.

The nature of $K^\pi = 4^+$ in deformed nuclei has been in discussion for a long time. The support for the 2056-keV $K^\pi = 4^+$ state in ^{168}Er as a two-phonon $\gamma\gamma$ excitation is based on the $B(E2)$ ratio $R(4^+) = B(E2,4_{\gamma\gamma} \rightarrow 2_\gamma)/B(E2,2_\gamma \rightarrow 0_g) \geqslant 1.1$ derived from lifetime data by Borner *et al.* [47], besides the anharmonicity estimates from various theoretical models. From the Coulomb excitation (CE) work [48], $B(E2,4_{\gamma\gamma} \rightarrow 2_\gamma) = 0.060(15)\, e^2b^2$ and the ratio $R(4^+)$ is 1.9(4). In DPPQM, Gupta *et al.* [49] predicted $R(4^+) = 2.5$

TABLE X. $B(E2)$ ratios for transitions from $K^\pi = 4_1^+$ $(\gamma\gamma)$ $I = 5, 6$ spins in ^{154}Gd.

I_i I_f/I_f'	$E_\gamma/E\gamma'$ (keV) [13]	I_γ/I_γ' [13]	$B(E2)$ ratio Expt. [9,11]	$B(E2)$ Expt. [13]	DPPQ 5_2^+	DPPQ 5_3^+
1770.2 keV						
5^+ $4_\gamma/4_{k=4}$	506.4/124.4	93/21	0.0012	0.004 1	0.06	0.20
$4_\gamma/4_\beta$	506.4/722.6	93/26	9.1 40	21 9	1.6	5.2
$4_g/4_\beta$	1400/722.6	11/26		0.015 9	0.001	0.002
$4_\gamma/3_\gamma$	506.4/642.4	93/100	2.8 5	3.1 6	2.1	1.1
$5_\gamma/3_\gamma$	337.4/642.4	35/100	7 2	9 3	3.0	0.7
1911.5 keV					6^+	
$B(E2,6_4\text{-}4_4)$	$0.24 = 49$ W.u.			0.24[a]	0.63	
$B(E2\,6_4\text{-}5_\gamma)$	$0.015 = 3.1$ W.u.			0.015[a]	0.023	
6^+ $4_{K=4}/4_\gamma$	265.8/647.6	54/71		65 13	498	
$5_\gamma/5_{K=4}$	479.2/141.3	52/100		0.0012 2	0.057	
$4_{K=4}/5_{K=4}$	265.81/141.3	54/100		0.023 3	1.3	
$4_\beta/4_\gamma$	545.7/647.6	8/71		0.26 11	0.30	
$4_g/4_\gamma$	1541.2/647.6	5.7/71		0.001 1	0.26	
$6_g/6_\gamma$	1193.3/304.8	41.6/19.5		0.0023 4	0.037	
$6_\gamma/5_\gamma$	304.8/479.2	19.5/52	3.5 8	3.6 5	1.6	

[a]Estimated by Wu *et al.* [19].

TABLE XI. $B(E2)$ ratios for transitions from $K^\pi = 2^+$ ($\beta\gamma$), $I^\pi = 2^+$ 1531.3 keV. 2^+_5 state in ^{154}Gd.

I_i I_f/I'_f	$E_\gamma/E\gamma'$ (keV)	I_γ/I'_γ [13]	Expt. [9,54]	Expt. [13]	DPPQ
$2_5(\beta\gamma)1531$					
$0_3/0_\beta$	349.2/850.6	2.96/100		2.54 10	2.0
$0_\beta/0_g$	850.6/1531.3	100.0/2.64	713 51	716 30	550
$2_\beta/2_g$	715.5/1408.2	76.9/10.2	246 36	223 15	7.1
$2_\gamma/2_g$	535.1/1408.2	7.0/10.2		87 8	6.6
$0_g/2_g$	1531.3/1408.2	2.64/10.2	0.17 4	0.17 2	0.01
$4_g/2_g$	1160.5/1408.2	19.0/10.2	4.86 73	4.90 30	0.1
$0_\beta/2_\beta$	850.6/715.8	100.0/76.9	0.55 2	0.55 2	1.0
$4_\beta/2_\beta$	483.7/715.8	3.86/76.9	0.20 5	0.36 2	1.6
$3_\gamma/4_\gamma$	403.5/267.4	9.2/1.58	0.25	0.74 7	0.95
$3(\beta\gamma)$ 1661					
$2_\beta/2_g$	845.4/1537.8	100/10.12	219 11	197 8	368
$4_\beta/4_g$	613.3/1289.9	16.4/3.70	333 19	182 9	140
$4_\gamma/4_g$	397.1/1289.9	4.86/3.70	943 53	572 32	365
$2_\gamma/2_g$	664.7/1537.8	4.60/10.12	38.4	30 2	50
$2_\beta/2_\gamma$	845.4/664.7	100/4.60	5.7 3	6.5 4	7.3
$4_\beta/4_\gamma$	613.3/397.1	16.4/4.86	0.35 2	0.38 2	0.38
$4_g/2_g$	1289.9/1537.8	3.70/10.12	0.55 13	0.88 3	1.1
$4_\beta/2_\beta$	613.3/845.4	16.4/100	0.84 4	0.82 4	0.7
$4_\gamma/2_\gamma$	397.1/664.7	4.86/4.60	13.6 8	13.8 7	13
$2_{\beta\gamma}/2_\gamma$	129.6/664.7	0.28/4.60		216 36	188
$2_{\beta\beta}/2_\gamma$	242.9/664.7	0.72/4.60		26 3	12
4 $(\beta\gamma)1789$					
$4_\beta/4_g$	740.9/1417.9	19/100		5 1	83
$2_g/4_g$	1665.8/1417.9	38/100	0.26 5	0.17 2	0.31
$6_g/4_g$	1071.2/1417.9	4.6/100	<5.7	0.19 4	0.8

in agreement with CE data. Similarly, measured $R(4^+) = (0.5-3.9)$ for ^{164}Dy [50] for 2173.1-keV 4^+ supports the $4_{\gamma\gamma}$ interpretation. For ^{154}Gd, no lifetime or Coulomb excitation data are available for the $K^\pi = 4^+$ state at 1646 keV.

The absolute $B(E2,4_{\gamma\gamma} \rightarrow 2_\gamma)$ in the DPPQM of $0.047\,e^2b^2$ or $\sim$9 W.u. compared to $B(E2,2_\gamma \rightarrow 0_g) = 0.029\,e^2b^2$ or $\sim$6 W.u. yielding $R(4^+) = 1.6$, and $B(E2,4_\gamma\text{-}2_g) = 0.015$ or 3 W.u. indicates good collectivity. Wu *et al.* estimated $B(E2,6_4\text{-}4_4) = 0.24\,e^2b^2$ or 49 W.u. (the DPPQM value exceeds this; Table X), which supports the collective structure of the $K^\pi = 4^+$ band. If one assumes a contribution of 2 quasiparticle components, the $B(E2)$ value will be less than one W.u. [19]. The energy levels (up to $I^\pi = 9^+$) of this band display a rotational pattern as for the ground band [19,13]. The above stated (Tables IX and X) preferential decays of all levels of the $K^\pi = 4^+$ band to the $K^\pi = 2^+$ γ band support the view of calling it a 2γ band.

In an alternative approach, Burke [51] on the basis of $E4$ strengths, and single-nucleon-transfer results, suggested the $K^\pi = 4^+$ band as predominantly hexadecapole vibrations. Ronnigen *et al.* [52] measured the $E4$ component in the ground band of $^{154-160}$Gd isotopes, yielding a small fraction of the quadrupole strength. For the excited bands, this admixture of $E4$ component should be smaller. Thus a small $E4$ admixture in the $K^\pi = 4^+$ is possible, along with the two phonon components.

Wu *et al.* [19] studied the problem of large anharmonicity in the energy of the $K = 4$ band versus the $K = 2$ band, the ratio $R = E(4_{\gamma\gamma})/E(2_\gamma)$ being $= 1.65$ in ^{154}Gd, lower than 2.0 expected for a harmonic 2γ-phonon band. The problem of energy anharmonicity in the 16 nuclei in Gd-Hf studied in [19] is rather complex and it varies with N and Z. Wu *et al.* [19] suggested that a greater γ-β separation leads to a higher value of the ratio R. On the basis of $\Delta E(\beta\text{-}\gamma)$, the ratio R falls in two groups. For $E(2_\beta) > E(2_\gamma)$, R is greater than 2.0 and for low 2_β, $R < 2.0$. In Gd isotopes, at $N = 90$ in ^{154}Gd, 2_β is below 2_γ In ^{156}Gd, $\Delta E(\beta\text{-}\gamma)$ is reduced, and in ^{158}Gd there is a crossover. The ratio R reduces from 1.6 to 1.34 in ^{156}Gd, and then increases to 1.52 in ^{158}Gd.

In Dy isotopes, the ratio R varies from 2.0 to 1.75, 1.73, and 2.85 for $N = 92$ to $N = 98$. However, at $N = 92$, 2_β just crosses over 2_γ and thereafter, 2_β moves up and 2_γ moves down continuously. Thus, its behavior is different from that of Gd isotopes. In $^{160\text{-}168}$Er isotopes, the ratio R increases monotonically from 1.89 through 2.98, 2.52, 2.60 at $N = 94-98$ to 2.65 at $N = 100$ and $\Delta E(\beta\text{-}\gamma)$ increases from $N = 92$ to 98, but the increase in R at $N = 100$ is not related to the decrease in $\Delta E(\beta\text{-}\gamma)$. Thus the relation of the anharmonicity R to $\Delta E(\beta\text{-}\gamma)$ seems to be partially valid. Three body interaction in the IBM has been used to obtain the anharmonicity in the ratio R for ^{166}Er in Ref. [53], with partial success. A major difference of the Gd isotopes from the Dy and Er isotopes is in the value of R, being less than 2, while most multiphonon theories [47] predicted $R > 2$.

Variations of R and $\Delta E(\beta\text{-}\gamma)$ with N and Z are related to more microscopic factors at play. In the microscopic approach

of dynamic PPQ model, a fair reproduction of the basic decay pattern is reproduced. Also in DPPQM, the ratio R for ^{154}Gd is close to the experimental value. This should justify the $K = 4$ band to be labeled as a two γ-phonon $\gamma\gamma$ band along with strong mixing with the γ band and β band, even if a small $E4$ component is present.

4. $K^\pi = 2^+$ $\beta\gamma$ band at 1531 keV

The revised $B(E2)$ ratios (column 5) for $E2$ transitions from the $K = 2$ $\beta\gamma$ band are almost the same as used earlier in [9] (column 4) in Table XI. The well established 1531-keV $2_{\beta\gamma}$ level in the decay scheme of ^{154}Gd is predicted to have a $(21 + 79)\%$ $K = 0, 2$ component admixture. Kulp *et al.* [15] assigned the 349.2-keV γ ray to populate the newly assigned 1182.2-keV 0_3^+ level from the $2_{\beta\gamma}$ state. The $B(E2)$ ratio relative to the 0_β^+ state agrees with the DPPQ model value (Table XI). Stronger decays to 0_β, 2_β, and 2_γ than to the g band are also given in DPPQM. The other $B(E2)$ ratios involving two levels of the same band also are reasonably well predicted (except for 4_g) in our calculation. DPPQM values of $B(E2, 2_5^+ \rightarrow 4_\gamma) = 0.10\, e^2b^2$ and $B(E2, 2_5^+ \rightarrow 0_3^+) = 0.05\, e^2b^2$ indicate coupling with the γ and 0_3 bands.

The predominant decay from the $3_{\beta\gamma}$ (1661-keV) state to members of β and γ band are indicated in theory as well. Other $B(E2)$ ratios also are given reasonably well in theory. The same trend is apparent for $4_{\beta\gamma}$ as well. The tentative assignment of 1789-keV $4_{\beta\gamma}$ was made from the 1417-keV $4_{\beta\gamma}$-4_g firmly assigned in coincidence [12], and is supported by the 1071.2-keV γ ray to 6_g, and other $E2$ transitions. The 4_6^+ in the DPPQM with $(9 + 63 + 28)\%$ $K =$ 0-, 2-, and 4-component admixture in the DPPQM is associated with this state, which gives reasonable $B(E2)$ ratios (Table XI). Thus we get an overall reasonable agreement from theory of the basic pattern of decay from the members of the $2_{\beta\gamma}$ band at 1531 keV in ^{154}Gd.

Kulp *et al.* [15] cited DPPQ results in [9] for this band, but expressed the need of fresh analysis. The transition quadrupole moments obtained from the relative $B(E2)$ values divided by Clebsch Gordan coefficients for E_γ from the levels in the $K = 2_2$ band showing an increase with final spin indicated band mixing with lower bands [15]. As stated above, $2_{\beta\gamma}$ has a large $(21 + 79)\%$ $K = 0$, 2 component admixture, and the $B(E2)$ ratios also indicate good mixing with β and γ bands. The PEC also indicates the mixture of prolate, oblate, and spherical shapes (Fig. 4). The $H_{\rm coll}$ includes the full (β, γ) dependence in the kinetic terms $T_{\rm rot}(\beta, \gamma)$ and $T_{\rm vib}(\beta, \gamma)$ terms, the latter involving the $B_{\beta\beta}$, $B_{\gamma\gamma}$, and $B_{\beta\gamma}$ mass coefficients. Thus it well qualifies to be the $K = 2$ $\beta\gamma$ vibrational band.

5. $K^\pi = 0_4^+$ (2γ) band

Sousa *et al.* [11] had assigned a 2081.0-keV level to $(2,3,4)^+$ on the basis of energy fits, and a 2230-keV level to $(2,3,4)^+$ on the basis of coincidence relations. But, in the NDS, 110 (2009) [14] and in [15], these assignments are replaced by 1573.97 keV (0^+), 1716.1 keV (2^+), and 2080.2 keV (4^+). Accordingly, the calculated $B(E2)$ ratios from these levels of the $K^\pi = 0_4^+$ band (which may be called 2γ $K = 0_4^+$ band) are listed in Table XII and compared with DPPQM results. The state 2_6^+ with 96% $K = 0$ component is associated with 1716-keV 2^+. The 4_7^+ of the DPPQM is associated with the 2080.2-keV $4_{K=04}$ state.

The 1574-keV 0_4^+ level decays preferentially to 2_γ versus 2_β and weakly to 2_g. Thus the $B(E2)$ ratio supports the $K^\pi = 0^+$ 2γ assignment. The $B(E2)$ ratios from other states of the band also support its collective nature. The intraband transition of 4_{04} to 2_{04} of 364.3 keV supports the 2080-keV 4^+ assignment. The 434-keV transition to $K = 4$ 1646-keV state yields a large $B(E2)$ ratio. Thus the assignments in this band seem reasonable. The DPPQ model calculation with sixth 2^+ (95% $K = 0$ component), and seventh 4^+ yields reasonable $B(E2)$ ratios corresponding to data (Table XII), with some ratios far off too.

The 2γ and 3β respective assignment to 0_4^+ and 0_5^+ bands is supported by the pattern of $B(E2)$ data (Tables XII and XIII), in comparison to a possible suggestion of regarding the 0_4^+ or 0_5^+ states as a 2β multiphonon state [15]. The smaller collectivity in 0_4^+ and 0_5^+ bands compared to the 0_3^+ band, as reflected in the intraband transitions $(2^+ \rightarrow 0^+) \sim 0.2\, e^2b^2$ versus $0.5\, e^2b^2$ in the DPPQM, do not support the suggestion put forth by Kulp *et al.* [15].

6. $K^\pi = 0_5^+$ band

The 0_5^+ state at 1650.34 keV decays predominantly to the 2_β level at 815.5 keV compared to the 2_g level, with the $B(E2)$ ratio ~5.5 (Table XIII). The 1775.4-keV 2^+ level decays to the g band ($I = 0,2,4$), 0_β ($I = 0,2,4$) band, and to the 3_γ level. The DPPQM values for 2_7^+ are listed in Table XIII. The preferential decay of 2_{05}^+ to 0_2^+ is given in the DPPQM, though with a larger ratio. *Also, the decays to the* g, β, and γ *band from the* 2_{05}^+ *state are of the order of* $0.01\, e^2b^2$ *and yield varied agreement with data*. The stronger decay of 1650-keV 0_5^+ to 2_2 is also not reproduced in the DPPQ model. The intraband $B(E2, 2_{05} \rightarrow 0_5)$ is only $0.24\, e^2b^2$, the same for $B(E2, 2_{04} \rightarrow 0_4)$, compared to $B(E2, 2_{04}^+ \rightarrow 0_3^+)$ of $0.63\, e^2b^2$ in the DPPQM.

TABLE XII. $B(E2)$ ratios for transitions from 1574.0 keV, $K^\pi = 0_4^+$ (2γ)-band in ^{154}Gd.

Transitions I_i I_f/I_f'	$E_\gamma/E\gamma'$ [13]	I_γ/I_γ' [13]	$B(E2)$ ratios Expt. [13]	DPPQ
$1573.97 = 0_4^+$				
0_4 $2_\gamma/2_\beta$	577.7/758.5	85.3/100	3.3 2	308
$2_g/2_\beta$	1451.7/758.5	27/100	0.011 3	3.4
1716.1 keV				
2_{04} $2_g/4_g$	1593.4/1345.0	75/100	0.32 21	0.29
$0_g/2_g$	1715.7/1593,4	60/75	0.6 4	0.001
$2_\gamma/2_g$	719.8/1593,4	45/75	32 18	200
$3_\gamma/2_\gamma$	588.3/719.8	73/45	4.5 9	5.0
2080.2 keV				
4_{04} $3_{\beta\gamma}/2_{04}$	419.3/364.3	9.5M1/3.2		1.2
$2_\gamma/3_\gamma$	1084.3/952.4	751/00	0.39 8	0.02
$4_{\gamma\gamma}/4_g$	434.4/1709.7	6.9/47	139 62	38
$4_g/6_g$	1709.7/1363.1	47/71	0.21 5	
$2_{04}/2_\gamma$	364.3/1084.3	3.2/75	10 4	5380

TABLE XIII. $B(E2)$ ratios for transitions from 1650.34 keV, $K^\pi = 0_5^+$ band in ^{154}Gd. No previous data were available in (1979) Ref. [9].

I_i I_f/I'_f	$E_\gamma/E\gamma'$ keV	I_γ/I'_γ [13]	$B(E2)$ ratios Expt. [13]	DPPQ
$1650.3 = 0_5^+$				
0_5^+ $2_2/2_1$	834.8/1650.3	17/100	5.5 19	0.1
1775.4 keV				
2^+ $0_2/0_1$	1094.9/1775.7	21/46	5.1 13	34
$0_1/2_1$	1775.7/1652.4	46/100	0 32 6	0.10
$4_1/2_1$	1404.6/1652.4	40/100	0.90 19	0.07
$2_2/4_2$	960.1/727.8	9/15	0.15 6	0.40
$3_1/4_2$	647.7/727.8	3/15	0 36 18	4.5

V. DISCUSSION AND SUMMARY

After referring briefly to the new works related to ^{154}Gd in the last four decades, in Sec. II we have reviewed the new data on its level scheme. Major changes have been reported on the levels of the excited $K^\pi = 0^+$ bands. Even if there is agreement on the nature of the $K^\pi = 0_2^+$ band in ^{154}Gd (after differing views for long), there remains an issue of different interpretations on the higher $K^\pi = 0^+$ bands. New data on $K^\pi = 0_{3,4,5}{}^+$ bands and other higher bands in ^{154}Gd are reviewed. In Sec. III, we have reviewed the salient features of the four decades old dynamic PPQ model. While the DPPQM has been successful in explaining the general features of shape transitional nuclei, the problem of energy scale of vibrational bands remains, as pointed out above. In a further development of the microscopic theory, Kumar (and co-workers) developed the dynamic deformation model (DDM) [36] using the Strutinsky shell correction method, replacing the use of Nilsson single particle orbits, which overcomes some of the problems of DPPQM. But the use of parameters free process produces its own limitations. Also, in the DPPQM one uses the Bohr Mottelson unified collective model for predicting the nuclear structure, unlike some other theories, based on the collective aspects of the shell model itself.

In Sec. IV, first we have compared the data on *absolute* $B(E2)$ *values* with the DPPQ model, which validates the model and the implied collectivity of the lower three bands. The data on $B(E2)$ ratios, intraband and interband, are compared with IBM and $X(5)$ symmetry in the tables. Agreement is better for stronger $E2$ transitions, and deviations are larger for weak $E2$ transitions. In many cases IBM and $X(5)$ predictions also are good. The PES of ^{154}Gd is given, which illustrates the prolate, oblate, and spherical shape mixings in the higher bands.

At respective places we have reviewed the different views on the nature of the excited bands, in relation to their vibrational and multiphonon interpretations. The low energy of β vibration in ^{154}Gd and other $N = 90$ isotones allows the formation of multiphonon bands at low energy. The differing views in [24–31] on the shape coexistence of the β band and ground band are discussed in Sec. IV D. The views as prevalent in the literature for higher lying bands have been reviewed. The very existence of regular collective bands in ^{154}Gd favors the collective multiphonon view of these bands, in spite of the anharmonicities which arise on account of the band mixings. Note the order of the different K bands related to the low 0_β and higher 2_γ states. In deformed isotopes of Gd and Dy, problems of reproducing even the β band versus the γ band (in 2^+ and higher spin states) in proper order arise (e.g., see [55] for ^{158}Dy).

The 2β phonon versus pairing vibration view is reviewed in some detail in Sec. IV E 2. The $2n$ transfer reactions indicate an admixture of pairing and quadrupole vibrations may be present. The problem of higher excited 0^+ states has a long history and is currently of great interest [44]. The $E(0_3^+)$ versus $E(0_2^+)$ ratio also varies widely with N and Z, and the anharmonicity alone does not explain this variation. Then one resorts to other alternatives, like single particle admixture or pairing vibration, etc. In fact the same problem occurs for $K^\pi = 4^+$ bands also, as discussed above in Sec. IV E 3, where, besides the Wu *et al.* [19] analysis for ^{154}Gd, we have cited the $K^\pi = 4^+$ bands of ^{168}Er and ^{164}Dy and the alternative view of $E4$ admixture in Burke's work [51]. The DPPQM results (Tables IX and X) support the collective aspects of the $K^\pi = 4^+$ band. It is possible for a small $E4$ component to be present in the 2γ band.

There is a view that $2n$ transfer reactions provide more microscopic information on the spectral features. This information also varies with N and Z. It is true that one cannot rely on the level energy and $B(E2)$ ratio data alone. But the information on collectivity may not be ignored either. The absolute $B(E2)$ values obtained in multiple Coulomb excitation and lifetime data, where possible, can provide additional support on collectivity. $E0$ transition strength data can provide additional information. The view of pairing isomer needs to be supported by a possible change of deformation (shape coexistence) for those states in the the overall spectrum. We have illustrated the different views as in Refs. [18,21,30,42–45]. As noted by Kumar in [21] one needs to compare the fluctuations in the pairing field and the quadrupole collective field in order to justify either view. The recent works on $2n$ transfer using s^+ and s operators of IBM in [30,45] have merit and further progress in this direction will be useful.

Also, 2γ $K = 0,2,4$ combinations of the three bands have different anharmonicities, as expected. This also remains an open problem for further experimental and theoretical developments. The lifetime data for these states can help to determine the nature of these states. In theory as well, an estimate of the $E4$ component, in addition to the $E2$ component (e.g., in g-boson IBM) can help in determining the predominant 2γ component in the $K^\pi = 4^+$ band.

The microscopic collective model approach in dynamic PPQ treatment accounts not only for the shape degrees of freedom but also the variation in the kinetic coefficients. This allows such a large number of data on the eight bands to be compared with experiment, even if the agreement is not close always. The spectrum of ^{154}Gd with eight collective bands, analyzed previously in (1979), and updated now after four decades, demonstrates the validity of the DPPQ model and of its predictive power on collective states. Kumar *et al.* have pointed out earlier [9] that in the dynamic deformation theory of Kumar-Baranger, each state has full freedom on its shape and kinematics. Also two and four quasiparticle excitations are already included in the treatment of the kinetic coefficients of the rotational, β-, and γ-vibration terms. However, the DPPQ model, while it gives extensive agreement with data, is giving only a partial reproduction of all the experimental data, so a more complete understanding of all the experimental data is needed. It would be helpful to have measurements of more lifetimes of excited states and $E0$ transitions to more fully understand the structure of ^{154}Gd.

ACKNOWLEDGMENTS

J. B. Gupta appreciates the postretirement association with Ramjas College, University of Delhi. The work at Vanderbilt University was supported by the U.S. Department of Energy under Grant No.DE-FG02-88ER40407.

[1] F. Iachello, Phys. Rev. Lett. **87**, 052502 (2001).
[2] D. Tonev, A. Dewald, T. Klug, P. Petkov, J. Jolie, A. Fitzler, O. Möller, S. Heinze, P. von Brentano, and R. F. Casten, Phys. Rev. C **69**, 034334 (2004).
[3] R. F. Casten and N. V. Zamfir, Phys. Rev. Lett. **87**, 052503 (2001).
[4] R. Krucken *et al.*, Phys. Rev. Lett. **88**, 232501 (2002).
[5] M. A. Caprio *et al.*, Phys. Rev. C **66**, 054310 (2002).
[6] A. Bohr and B. R. Mottelson, *The Nulear Structure Vol. II* (W. A. Benjamin, New York, 1975).
[7] F. Iachello and A. Arima, *The Interacting Boson Model* (Cambridge University Press, Cambridge, England, 1987).
[8] K. Kumar and M. Baranger, Nucl. Phys. A **110**, 529 (1968).
[9] K. Kumar, J. B. Gupta, and J. H. Hamilton, Aust. J. Phys. **32**, 307 (1979).
[10] J. H. Hamilton, Bull. Russian Acad. Sci. Phys. Ser. **36**, 17 (1972).
[11] D. C. Sousa, L. L. Riedinger, E. G. Funk, and J. W. Mihelich, Nucl. Phys. A **238**, 365 (1975).
[12] J. B. Gupta, S. L. Gupta, J. H. Hamilton, and A. V. Ramayya, Z. Phys. A **282**, 179 (1977).
[13] Brookhaven National Laboratory, Chart of nuclides of National Nuclear Data Center, http://www.nndc.bnl.gov/ENSDF.
[14] C. W. Reich, Nucl. Data Sheets **110**, 2257 (2009).
[15] W. D. Kulp, J. L. Wood, K. S. Krane, J. Loats, P. Schmelzenbach, C. J. Stapels, R.-M. Larimer, and E. B. Norman, Phys. Rev. C **69**, 064309 (2004).
[16] R. A. Meyer, Phys. Rev. **170**, 1089 (1968).
[17] R. Bloch, B. Elbek, and P. O. Tjom, Nucl. Phys. A **91**, 576 (1967).
[18] W. D. Kulp, J. L. Wood, K. S. Krane, J. Loats, P. Schmelzenbach, C. J. Stapels, R.-M. Larimer, and E. B. Norman, Phys. Rev. Lett. **91**, 102501 (2003).
[19] X. Wu, A. Aprahamian, S. M. Fischer, W. Reviol, G. Liu, and J. X. Saladin, Phys. Rev. C **49**, 1837 (1994).
[20] K. Kumar, in *The Electromagnetic Interaction in Nuclear Physics*, edited by W. D. Hamilton (North-Holland, Amsterdam, 1975), Chap. 3.
[21] K. Kumar, Nucl. Phys. A **231**, 189 (1974).
[22] N. N. Bogoliubov, Usp. Fiz. Nauk. **67**, 549 (1959).
[23] O. Scholten, Computer program package PHINT KVI Internal Report, 1979.
[24] N. V. Zamfir, R. F. Casten, M. A. Caprio, C. W. Beausang, R. Krucken, J. R. Novak, J. R. Cooper, G. Cata Danil, and C. J. Barton, Phys. Rev.C **60**, 054312 (1999).
[25] P. E. Garrett, J. Phys. G **27**, R1 (2001).
[26] P. Debenham and N. M. Hintz, Nucl. Phys. A **195**, 385 (1972).
[27] J. Jolie, P. Cejnar, and J. Dobes, Phys. Rev. C **60**, 061303 (1999).
[28] D. G. Burke, Phys. Rev. C **66**, 024312 (2002).
[29] R. M. Clark, M. Cromaz, M. A. Deleplanque, R. M. Diamond, P. Fallon, A. Gorgen, I. Y. Lee, A. O. Macchiavelli, F. S. Stephens, and D. Ward, Phys. Rev. C **67**, 041302(R) (2003).
[30] R. M. Clark, R. F. Casten, L. Bettermann, and R. Winkler, Phys. Rev. C **80**, 011303(R) (2009).
[31] J. B. Gupta and J. H. Hamilton, Eur Phys. J. A **51**, 151 (2015).
[32] Z. P. Li, J. Xiang, J. M. Yao, and H. Chen, Int. J. Mod. Phys. E **20**, 494 (2011).
[33] N. Pietralla and O. M. Gorbachenko, Phys. Rev. C **70**, 011304(R) (2004).
[34] R. Fossion, D. Bonatsos, and G. A Lalazissis, Phys. Rev. C **73**, 044310 (2006).
[35] Z. P. Li, T. Niksic, D. Vretenar, J. Meng, G. A. Lalazissis, and P. Ring, Phys. Rev. C **79**, 054301 (2009).
[36] K. Kumar, *Nuclear Model and Search for Unity in Nuclear Physics* (Universitetsforlaget, Bergen, 1984).
[37] K. Kumar (private communication).
[38] P. Van Isacker, P. O. Lipas, K. Helimaki, I. Koivistoinen, and D. D. Warner, Nucl. Phys. A **476**, 301 (1988).
[39] R. Bijker, R. F. Casten, N. V. Zamfir, and E. A. McCutchan, Phys. Rev. C **68**, 064304 (2003).
[40] N. Rud, H. L. Nielsen, and K. Wilsky, Nucl. Phys. A **167**, 401 (1971).
[41] L. L. Riedinger, J. H. Hamilton, and N. R. Johnson, Phys. Rev. C **2**, 2358 (1970).
[42] M. A. M. Shahabuddin, D. G. Burke, I. Nowikow, and J. C. Waddington, Nucl. Phys. A **340**, 109 (1980).
[43] I. Ragnarsson and R. A. Broglia, Nucl. Phys. **263**, 315 (1976).
[44] D. A. Meyer *et al.*, Phys. Rev. C **74**, 044309 (2006).
[45] R. Fossion, C. E. Alonso, J. M. Arias, L. Fortunato, and A. Vitturi, Phys. Rev. C **76**, 014316 (2007).
[46] J. B. Gupta, Phys. Rev. C **87**, 064318 (2013).
[47] H. G. Borner, J. Jolie, S. J. Robinson, B. Krusche, R. Piepenbring, R. F. Casten, A. Aprahamian, and J. P. Draayer, Phys. Rev. Lett. **66**, 691 (1991).
[48] T. Härtlein, M. Heinebrodt, D. Schwalm, and C. Fahlander, Eur. Phys. J. **A2**, 253 (1998).

[49] J. B. Gupta, J. H. Hamilton, and A. V. Ramayya, Phys. Rev. C **63**, 044308 (2001).
[50] F. Corminboeuf, J. Jolie, H. Lehmann, K. Fohl, F. Hoyler, H. G. Borner, C. Doll, and P. E. Garrett, Phys. Rev. C **56**, R1201 (1997).
[51] D. G. Burke, Phys. Rev. Lett. **73**, 1899 (1994).
[52] R. M. Ronningen *et al.*, Phys. Rev. C **16**, 2208 (1977).
[53] J. E. García-Ramos, C. E. Alonso, J. M. Arias, and P. Van Isacker, Phys. Rev. C **61**, 047305 (2000).
[54] D. R. Zolnowski, E. G. Funk, and J. W. Mihelich, Nucl. Phys. A **177**, 513 (1971).
[55] J. B. Gupta, Int. J. Mod. Phys. E **25**, 1650076 (2016).